

# The Perceived Roughness of Resistive Virtual Textures: II. Effects of Varying Viscosity with a Force-Feedback Device

SUSAN J. LEDERMAN

Queen's University

ROBERTA L. KLATZKY

Carnegie Mellon University

and

CHRISTINE TONG and CHERYL HAMILTON

Queen's University

---

Klatzky and Lederman [2006] have shown that tangential resistive forces may be used to convey roughness in virtual textures using the WingMan force-feedback mouse. Modeling our experiment after this study, we directly examined the effect of viscous resistance on the perceived roughness magnitude of virtual gratings using a PHANTOM. For each virtual grating, the resistance level encountered at the ridges was varied by altering the viscosity coefficient. Perceived roughness systematically increased as the value of the viscosity coefficient was increased. The ridge-to-groove ratio contributed a small additional effect of microgeometry. These results suggest that simple models of viscous resistance may be used to simulate varying levels of surface roughness.

Categories and Subject Descriptors: H.5.1 [**Information Systems**]: Information Interfaces and Presentation—*Multimedia information systems*; H.5.2 [**Information Systems**]: Information Interfaces and Presentation—*User interfaces*

General Terms: Artificial, Augmented, and Virtual Realities, Evaluation/Methodology, Ergonomics, Haptics I/O, User-Centered Design, Experimentation, Human Factors, Performance

Additional Key Words and Phrases: Texture perception, virtual reality, haptics

---

## 1. INTRODUCTION

In the last 35 years the study of tactile texture perception has considerably increased as a result of the expanding multidisciplinary interest of researchers in the fields of psychophysics, neuroscience, and computational modeling. Early work emphasized texture perception with the bare finger, but with the development of force-feedback interfaces that allow virtual textures to be created, there is new interest in texture perception as mediated through a variety of mechanical linkages.

### 1.1 Texture Perception of Real Surfaces with the Bare Finger

Much of the early research on tactile texture perception via direct skin-surface contact has focused on the perception of surface roughness, one of the most prominent textural attributes. We will not

---

Authors' addresses: Susan J. Lederman, Christine Tong, and Cheryl Hamilton, Department of Psychology, Queens University, Kingston, Ontario, K7L 3N6; Roberta L. Klatzky, Department of Psychology, Carnegie Mellon University, Center for the Neural Basis of Cognition, Pittsburgh, PA 15213.

Permission to make digital or hard copies of part or all of this work for personal or classroom use is granted without fee provided that copies are not made or distributed for profit or direct commercial advantage and that copies show this notice on the first page or initial screen of a display along with the full citation. Copyrights for components of this work owned by others than ACM must be honored. Abstracting with credit is permitted. To copy otherwise, to republish, to post on servers, to redistribute to lists, or to use any component of this work in other works requires prior specific permission and/or a fee. Permissions may be requested from Publications Dept., ACM, Inc., 1515 Broadway, New York, NY 10036 USA, fax: +1 (212) 869-0481, or [permissions@acm.org](mailto:permissions@acm.org).  
© 2006 ACM 1544-3558/06/0100-0015 \$5.00

provide further details of this work in our introduction inasmuch as the current paper focuses on haptic roughness perception of virtual surfaces. For detailed descriptions, the reader should consult work by Katz [1925/1989], by Lederman and her colleagues [e.g., Taylor and Lederman 1975; Lederman 1983], by Johnson and his colleagues [e.g., Blake et al. 1997; Connor and Johnson 1992; Connor et al. 1990], and by Hollins and his colleagues [e.g., Hollins et al. 1998; Hollins and Risner 2000]. In brief, spatial encoding strongly influences roughness perception, particularly that of macrot textures (i.e., surfaces with interelement spacings greater than  $\sim 1$  mm); temporal factors are strongly implicated for micro textures with interelement spacings less than  $\sim 1$  mm [e.g., Hollins and Risner 2000; Hollins et al. 1998; LaMotte and Srinivasan 1991]. However, spatial coding has also been demonstrated with very finely textured surfaces [Yoshioka et al. 2001]. For real surfaces, a power function best describes the relation between perceived-roughness magnitude and interelement spacing.

### 1.2 Texture Perception of Real Surfaces with a Rigid Probe

We have also investigated the perception of surface roughness when a rigid intermediate link intervenes between the bare skin and the surface [Klatzky and Lederman 1999, 2002; Klatzky et al. 2003; Lederman et al. 2000, 1999]. The rigid links have included use of a pencil-like stylus with a spherical tip, a molded rigid sheath covering the volar surface of the most distal finger phalanx, and a probe designed to present vibrations to the finger tips with no force moments. Observers estimate the perceived-roughness magnitudes of textured surfaces consisting of raised, truncated cones or cylinders arranged as spatially jittered arrays. The interelement spacing is varied across the set of stimulus surfaces. The probe tip moves across the tops of the raised elements, sometimes falling between adjacent elements and moving across the smooth base when the probe-tip diameter is smaller than the interelement spacing. The mechanical vibrations produced by the interaction between probe tip and surface vary accordingly.

Over a series of studies (see above), we have found that the observed relation between apparent roughness magnitude and interelement spacing is quadratic. The magnitude of perceived-roughness grows as a function of interelement spacing, peaking at a point along the spacing axis that varies with probe-tip diameter and speed of relative motion. We proposed that the peak position along the interelement spacing axis falls close to the point at which the probe first begins to drop down between adjacent elements as opposed to moving across the tops of the elements (the “drop point”). The form of the psychophysical function relating log roughness magnitude to log interelement spacing thus depends upon the probe-tip size relative to the range of interelement spacing values. For relatively small or large probe tips, the function tends to monotonically increase or decrease, respectively; with a larger range that fully encompasses the drop point, the function is closer to a symmetric parabolic shape.

### 1.3 Rendering Surface Textures with a Haptic Interface and the Psychophysics of Virtual Textures

Researchers have begun to render textures by simulating point-contact interactions with virtual surfaces (e.g., gratings, grids, Perlin textures, and nontextured materials) using several different force-feedback devices and various rendering algorithms (i.e., two-, three-, and six-DoF). Unfortunately, the process of rendering surface textures raises several significant challenges which we have described in our companion paper. In brief, these include perceived instabilities at critical frequencies with some interfaces [Choi and Tan 2002, 2003; Champion and Hayward 2005, provide criteria for assessing the boundaries on rendering virtual haptic textures with haptic interfaces], the heavy computational demands [Siira and Pai 1996], and the high cost. In addition, relatively few papers have psychophysically evaluated those textures that have been rendered. An extensive description of the devices, rendering algorithms, and virtual texture psychophysics is presented in Klatzky and Lederman [2006].

#### 1.4 Motivation for the Current Study

In the accompanying Klatzky and Lederman study [2006], we investigated the role of microgeometry on the haptic roughness perception of virtual rectangular gratings generated with the WingMan force-feedback mouse (Immersion Corp.)—a low-cost haptic interface. We used a one-dimensional (1D) algorithm in which smooth regions alternated with resistive regions. In that study, we found that the width of the resistive patches (ridge width,  $R$ ) systematically accounted for the primary changes in perceived-roughness magnitude, as opposed to spatial period, groove width ( $G$ ) with zero resistance, or ridge-to-groove ratio ( $R:G$ ). The results of this study demonstrate the promise of using inexpensive devices to create virtual textures that can be freely explored.

In an effort to quantify the forces delivered by the mouse, Klatzky and Lederman [2006] found that it acted like a viscous device, in that the resistive force depended on velocity. The equation for this model is

$$F = -\gamma * v$$

where  $F$  and  $v$  are vectors and the minus sign indicates opposing directions.  $\gamma$  is a coefficient on velocity that affects the force, and thus can be called a viscosity coefficient or viscosity parameter. The units of  $\gamma$  are (N\*s)/mm. It must be noted, however, that the viscosity cannot be programmed definitively in the mouse and appears to vary to some extent with use. Hence, this device is inadequate for systematic testing of viscosity-produced roughness. The results of the WingMan study motivated us to conduct a more systematic investigation to determine whether viscosity, a velocity-dependent parameter, might influence the perceived-roughness of virtual textures using a force-feedback device with more precise control.

To date, we have found only one paper by Weisenberger et al. [2000] that is relevant to our study. Subjects were required to perform a two-alternative forced-choice task in which they judged the orientation of virtual gratings (horizontal or vertical) that were implemented using both the two-DoF Immersion IE2000 force-feedback stick and the three-DoF PHANTOM. With respect to the PHANTOM, the study directly compared two force models, one a damping model ( $F = b * v$ ), where  $b$  is the damping coefficient, and  $v$  the average velocity of movement, and the other a stiffness or spring model ( $F = k * x$ ), where  $k$  is the stiffness coefficient, and  $x$ , the position on the x axis. The results indicated that the damping model produced better performance than the spring model in a test of spatial acuity.

In the current study, we directly evaluate the potential of using a viscosity parameter to generate a range of perceived-roughness values. We used the Klatzky and Lederman algorithm for force, adapted for the PHANTOM Premium 1.0 haptic interface, a popular research tool that offers better control than the WingMan. We used the same range of geometric scale values as in the Experiment 2 of the WingMan study to generate a wide range of linear virtual rectangular gratings that were directly varied in ridge width and in ridge width:groove width ratio, with groove width covarying accordingly. In Experiment 1, we begin by exploring the effect of the viscosity coefficient using two extreme values on the viscosity-coefficient continuum that are usable with the PHANTOM. In Experiment 2, we further explore the effect of the viscosity parameter by extending the number of viscosity-coefficient values within the same range.

In brief, the current study reveals that a viscosity coefficient on velocity strongly influences the haptic estimation of the roughness magnitude of virtual gratings, an effect that appears to be secondarily dependent on grating microgeometry, and more specifically, on the ridge-to-groove ratio.

## 2. EXPERIMENT 1: THE ROLE OF VISCOSITY COEFFICIENT AND MICROGEOMETRY

In addition to evaluating the influence of the velocity-dependent parameter, viscosity coefficient, on the magnitude of perceived-roughness of rectangular gratings, we also manipulated two microgeometry

parameters (i.e., ridge width and ridge-to-groove ratio), with a third related parameter, groove width, which covaried with ridge-to-groove ratio. The contributions of all three parameters were assessed in our companion paper across a wide range of values that were used to produce virtual rectangular gratings. The three parameters and their associated values were drawn from Experiment 2 of our companion study.

## 2.1 Method

**2.1.1 Participants.** A total of 16 participants (5 males, 11 females) participated. Their mean age (SD) was 19.0 (0.6) years. Participants were drawn from the Introductory Psychology subject pool at Queen's University. They each received a credit toward their final grade for participating. Right-handed participants were selected, as determined from a brief questionnaire about hand usage in a set of five tasks (writing, drawing, throwing, using scissors, and using toothbrush), as defined by Bryden [1977].

**2.1.2 Apparatus and Virtual Textures.** A PHANTOM Premium 1.0 (SensAble) was used as the haptic interface. A variant of the WingMan algorithm above was adapted for use with the PHANTOM to produce linear rectangular gratings. The gratings were simulated as patterns of varying resistive force across a horizontal plane. More specifically, participants experienced a resistive force ( $\gamma * \text{velocity}$ ) when they traversed a virtual ridge and no resistance across the grooves. The parameter  $\gamma * \text{velocity}$  provides a viscous component of resistance, with  $\gamma$  being the viscosity coefficient. To ensure stability, speed was determined based on a moving average of the last three values of instantaneous velocity sampled at a frequency of 1 kHz. Note that resistance was always applied to directly oppose the participants' motion, that is, in a direction opposite that of the hand movement. The full range of viscosity-coefficient values that produced perceptually "good" gratings (i.e., with minimum instability) was employed, namely from 0.0013 to 0.0065 N\*s/mm.

Each virtual surface was divided into three sections. The two outer sections were smooth and the inner section consisted of linear rectangular gratings. The widths of the smooth and textured sections were 20 and 70 mm, respectively. The overall x and z dimensions of the planar stimulus surfaces in the coordinate frame of the PHANTOM were 110 mm  $\times$  25 mm, respectively.

On the monitor, the visual position of the stimulus was represented as a horizontal grey line, 110 mm long and 4 mm high. A red dot indicated the position of the probe as it was moved back and forth across the surface. Participants were instructed to explore the surface lightly, ensuring that the red dot moved left and right over the stimulus. Each trial began with the red dot on the smooth portion to the left of the inner textured area, as shown in Figure 1.

Six sets of gratings, each with a constant R:G ratio, were created. The ratio values ranged from 0.25 to 1.50, in increments of 0.25, as in Experiment 2 of the Klatzky and Lederman study [2006]. A wide range of R:G (0.25–1.50) and ridge width (R = 0.08, 0.16, 0.31, 0.62, and 1.25 mm) values were independently varied, thus allowing the groove width (G) value to vary accordingly, as shown in Table I.

We chose to manipulate ridge (as opposed to groove) width because our initial pilot work suggested that resistive ridge width might influence the perceived-roughness of the PHANTOM textures more than groove width. In addition, ridge width proved to be the single most important microgeometric parameter affecting perceived-roughness in our companion study [2006] with the WingMan force-feedback device.

**2.1.3 Experimental Procedure.** An absolute magnitude-estimation procedure was used to judge felt roughness. Participants were instructed to select the positive number (fraction, decimal, or whole number) that best described the perceived-roughness magnitude of each virtual surface. As in Klatzky and Lederman [2006], participants were instructed to judge roughness by imagining that they were in a car moving over a bumpy road. Participants were given a total of 24 practice stimuli, selected from the

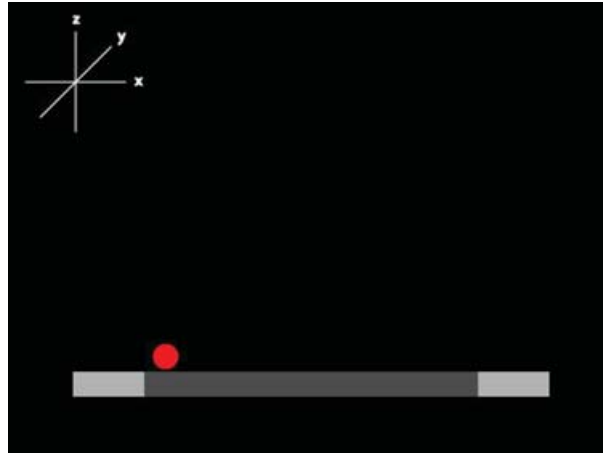


Fig. 1. Experiment 1: Participant view of the image shown on the computer monitor. The position of the surface is shown, with the outer smooth (light) and middle textured (dark) portions indicated. The changing contact position with respect to the virtual surface is indicated by movement of the cursor (dot) in both  $x$  and  $z$ . The  $x$ - $y$ - $z$  coordinate frame of the PHANTOM is shown at the top left, but is not visible to the participant.

ridge width and R:G values that were manipulated in the actual experiment on the basis of earlier pilot data. This selection procedure served to sample perceived roughness across the entire range observed in the pilot data. At the end of the experiment, which lasted approximately 50 min with a short break in the middle, the participants were asked to describe the cues used to make their roughness judgments.

**2.1.4 Experimental Design.** The experiment involved four within-subject factors, including R:G ratio with six levels (0.25, 0.5, 0.75, 1.0, 1.25, and 1.5), ridge width with five levels (0.08, 0.16, 0.31, 0.62, and 1.25 mm), viscosity coefficient with two levels (0.0013, 0.0039) and viscosity-coefficient block repetition with two levels. The viscosity-coefficient factor was blocked because in the pilot results randomizing this factor seemed to swamp possible effects due to other microgeometric factors. Participants received two repetitions of all  $R \times R:G$  combinations (60 trials) within both constant viscosity-coefficient blocks for a total of 240 trials. The 60 trials were completely randomized within each viscosity-coefficient block. The order in which the two viscosity-coefficient conditions were presented was counterbalanced across participants using four different orders.

## 2.2 Results

As in our previous work [e.g., Klatzky et al. 2003], the means of the magnitude estimates were calculated over all repetitions to provide more stable values for subsequent analysis. To eliminate any differences in the number scales used by individual participants, these values were then normalized by dividing each score by the participant's overall mean, and then multiplying by the grand mean calculated across participants. Finally, the normalized scores were logarithmically transformed to produce geometric means, which have been shown to produce less variability than arithmetic means [Stevens and Harris 1962].

These data served as input to a three-factor, within-subject ANOVA, the factors being R:G ratio (6), ridge width (5), and viscosity coefficient (2). Eta squared ( $\eta^2$ ) was used to compare the relative contributions of the main treatment effects. Unlike the results of our companion paper [Klatzky and Lederman 2006], the main effect of ridge width was not significant,  $F(1.546, 23.183) = 0.33$ ,  $\eta^2 = 0.001$ . The main effect of viscosity coefficient was highly significant,  $F(1, 15) = 117.95$ ,  $p < 0.0001$ :

Table I. Experiment 1: Microgeometry (mm) of Virtual Rectangular Gratings<sup>a</sup>

R:G	R	G
0.25	0.08	0.320
	0.16	0.640
	0.31	1.240
	0.62	2.480
	1.25	5.000
0.50	0.08	0.160
	0.16	0.320
	0.31	0.620
	0.62	1.240
	1.25	2.500
0.75	0.08	0.107
	0.16	0.213
	0.31	0.413
	0.62	0.827
	1.25	1.667
1.00	0.08	0.080
	0.16	0.160
	0.31	0.310
	0.62	0.620
	1.25	1.250
1.25	0.08	0.064
	0.16	0.128
	0.31	0.248
	0.62	0.496
	1.25	1.000
1.50	0.08	0.053
	0.16	0.107
	0.31	0.207
	0.62	0.413
	1.25	0.833

<sup>a</sup>R:G, ridge-to-groove ratio; R, ridge width; G, groove width.

perceived-roughness increased as the viscosity coefficient increased. The main effect of R:G ratio was also significant,  $F(1.56, 23.45) = 6.57, p < 0.001$ , with perceived-roughness again increasing as the R:G ratio increased. Because of an unintended error, two incorrect groove width values (and thus two incorrect R:G ratios) were used in the experiment. The note below<sup>1</sup> explains why we conclude that the unintended errors had little if any influence on the original pattern of results obtained. Accordingly,

<sup>1</sup>Unfortunately, during data analysis, we discovered that two of the stimulus gratings were produced with unintended groove width and corresponding R:G ratio values. Because it was not possible to perform an ANOVA with missing cells, we chose rather to perform two reduced repeated-measures ANOVAs to determine if the effects documented in the full original analysis were biased. The original three-factor, repeated-measures design, was retained in both analyses, and the data normalized accordingly. In the first reduced analysis, we eliminated the two affected ridge width levels ( $R = 0.16; 0.31$ ) that contained the faulty groove width values; thus, ridge width had three (not five) levels. In the second reduced analysis, we retained all five ridge-width values, but eliminated the two R:G ratio levels from the original six values that contained the wrong groove-width values. The two reduced analyses replicated the highly significant main effects of viscosity coefficient and R:G ratio. For each reduced ANOVA, of the two significant two-way interaction terms (viscosity coefficient  $\times$  ridge width and ridge width  $\times$  R:G ratio) that were significant in the original complete ANOVA, only the interaction term that involved the same number of levels as the original analysis remained statistically significant. Regardless, for both reduced ANOVAs, the magnitude of the significant effect due to the one significant interaction term, viscosity coefficient  $\times$  ridge width (0.015) was quite small. Accordingly, in Figure 2, we show only the consistently significant main effects due to viscosity coefficient and ridge-to-groove ratio based on the original data set.

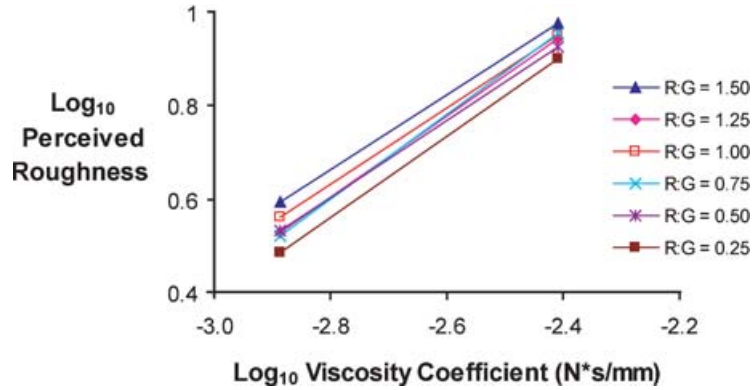


Fig. 2. Experiment 1: perceived roughness (means of the  $\log_{10}$  normalized roughness magnitude estimates) as a function of  $\log_{10}$  viscosity coefficient for each R:G ratio.

Figure 2 shows log normalized geometric means of the perceived-roughness estimates as a function of viscosity coefficient for each of the R:G ratio conditions, although the interaction of R:G ratio  $\times$  ridge width and viscosity  $\times$  ridge width were both marginally significant,  $F(3.35, 50.25) = 3.07$  and  $F(1.97, 29.48) = 3.36$ , both  $p < 0.05$ , respectively. The  $\eta^2$  values, shown in parentheses, indicate a very sizeable contribution of viscosity coefficient (0.622) and relatively small effects of the R:G ratio (0.012) and the interactions, R:G ratio  $\times$  ridge (0.016) and viscosity coefficient  $\times$  ridge width (0.008). As we shall see, the effect of R:G ratio is highly significant as well in Experiment 2 and so we consider its effect further. However, since the interaction effects are not consistently significant across experiments and because their corresponding  $\eta^2$  values are relatively very small, we will not discuss them again.

Because groove-width values covaried with R:G ratios, we next examined the log normalized geometric means of the roughness estimates as a function of the actual groove width corresponding to each R:G ratio condition, for all combinations of the viscosity coefficient and ridge width. These data are presented in Figure 3 (with the two groove-width conditions that were omitted in error). From the flat functions that are compressed along the ridge-width variations, we conclude that there is no influence of groove width or ridge width per se and, thus, that the R:G ratio itself—as opposed to either G or R—systematically influences the estimates of felt roughness magnitude.

A subjective questionnaire was presented at the end of the experiment to obtain information about the cues used to judge roughness and smoothness. The results were extremely consistent in that 15 of the 16 participants mentioned using resistance to estimate felt roughness, with greater resistances representing higher perceived-roughness estimates. The remaining participant mentioned deliberately attempting to ignore this cue in her judgments. In addition, some of the participants described the rougher surfaces as being bumpier, having fewer bumps, or that the bumps were more separated. We will discuss the results of Experiment 1 together with those of the next experiment in the general discussion.

### 3. EXPERIMENT 2: A FURTHER ASSESSMENT OF THE ROLES OF VISCOSITY COEFFICIENT AND MICROGEOMETRY

Experiment 1 revealed a strong effect of the velocity-dependent viscosity coefficient on the perceived magnitude estimates of virtual roughness. To assess the influence of this factor more thoroughly, we increased the number of values assigned to the viscosity-coefficient parameter from two to five within the

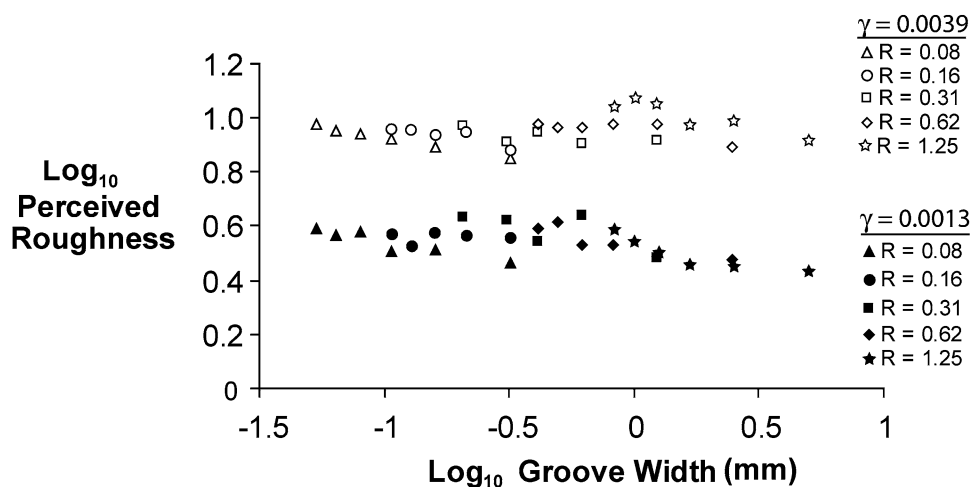


Fig. 3. Experiment 1:  $\text{Log}_{10}$  perceived-roughness (mean of  $\text{log}_{10}$  normalized roughness magnitude estimates) as a function of  $\text{log}_{10}$  groove width for all ridge-width  $\times$  viscosity coefficient ( $\gamma$ ) combinations.

range used in Experiment 1. We chose to vary ridge width (as opposed to R:G ratio) as in Experiment 1, because this factor clearly influenced perceived roughness in the Klatzky and Lederman [2006] study using the WingMan. To keep the total number of session trials manageable, we consequently limited the R:G ratio values to the minimum and maximum values used in Experiment 1. In addition, we recorded end-effector movements and forces for use in subsequent analyses.

### 3.1 Method

**3.1.1 Participants.** A total of 12 participants (2 males; 10 females) participated. Their mean age (SD) was 21.8 (1.7) years. Participants were paid \$10 for their participation. All participants were classified as right-handed according to the same criteria used in Experiment 1 [Bryden 1977].

**3.1.2 Virtual Texture Set.** The overall width of the display area was increased from 110 mm in Experiment 1 (i.e., 20 mm across the left smooth section, 70 mm across the central grating section, and 20 mm across the right smooth section) to 177.7 mm in Experiment 2 (i.e., left, central and flat regions of 50.8, 76.2, and 50.7 mm, respectively). As before, the stimuli extended the full length of the workspace along the z axis (i.e., 25 mm), in the coordinate frame of the PHANTOM.

As in Experiment 1, the stimuli consisted of five sets of constant-ridge-width gratings, each set consisting of five different viscosity coefficients (0.0013 to 0.0065, in increments of 0.0013  $\text{N}^*\text{s}/\text{mm}$ ), crossed with two R:G ratios (i.e., 0.25 and 1.50, with groove width varying accordingly). The corresponding grating specifications for Experiment 2 may be obtained from Table I.

The participant's view is the same as in Experiment 1 (Figure 1), with the exception that two windows were added to indicate the regions within which the participant was permitted to change movement direction.

**3.1.3 Experimental Procedure.** Participants were instructed to perform two complete exploratory cycles, starting on the left side of each stimulus (i.e., left-right, left-right) and to move at a comfortable speed. A 20-mm colored zone was displayed on the monitor immediately to the left and right of the central grating portion, up to a level of 30 mm above the stimulus (not shown in Figure 1). To clearly define the start and end positions of the trajectory, participants were required to switch directions

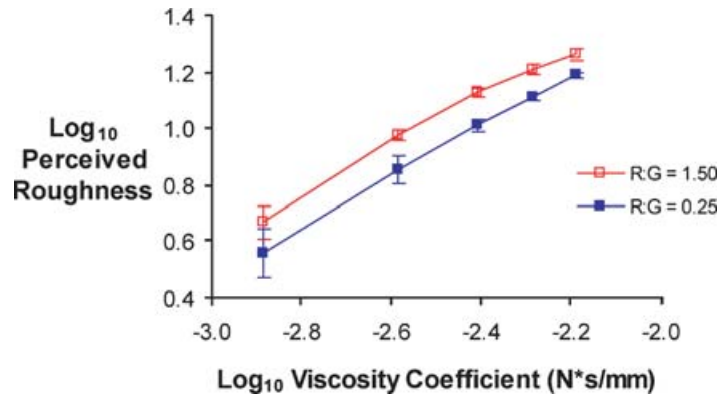


Fig. 4. Experiment 2: Log<sub>10</sub> perceived-roughness (mean log<sub>10</sub> normalized magnitude estimates) ( $\pm 1$  SEM) are shown as a function of viscosity coefficient for each R:G ratio.

within these zones. When this did not occur, an error message flashed on the monitor. The trial was then repeated at the end of the block.

Practice consisted of one full set of gratings presented at each of the five viscosity-coefficient levels to provide the participants with practice using numbers and to familiarize them with moving the probe at a comfortable speed. They were told that they could refine their choice of numbers following practice, but that they should be consistent in their numeric judgments across the formal experiment. One extremely slow participant was eliminated because he had only completed one-third of the trials by the end of the session. When the experiment ended, participants were asked to describe the cues they had used to make their roughness estimates.

**3.1.4 Experimental Design.** A within-subject design was used in which each participant judged the roughness magnitude of 50 stimuli, representing the complete crossing of five viscosity-coefficient values  $\times$  five ridge-width values  $\times$  two R:G values. Each combination was repeated four times. The order in which the gratings were presented within each repetition was fully randomized.

## 3.2 Results

As in Experiment 1, we began by averaging the magnitude estimates across repetitions. A three-factor, within-subject ANOVA was performed on the log<sub>10</sub> normalized magnitude estimates with the factors being viscosity-coefficient (five levels: 0.0013, 0.0026, 0.0039, 0.0052, and 0.0065 N\*s/mm), ridge width (five levels: 0.08, 0.16, 0.31, 0.62, and 1.25 mm), and R:G ratio (two levels: 0.25, 1.50).

The main effect of ridge width was not significant,  $F(1.43, 15.78) = 0.38, p > 0.05; \eta^2 = 0.0006$ . The effect of viscosity-coefficient was highly significant,  $F(1.07, 11.78) = 51.82, p < 0.0001$ , as was the effect of R:G ratio,  $F(1, 11) = 14.26, p < 0.005$ . As in Experiment 1, the log<sub>10</sub> normalized perceived-roughness estimates increased with increasing values of log<sub>10</sub> viscosity-coefficient and R:G ratio. The effects are presented in Figure 4, which shows log<sub>10</sub> normalized geometric mean roughness estimates as a function of the viscosity-coefficient for both R:G ratios.<sup>2</sup> The  $\eta^2$  values for these two factors were 0.687 and 0.038, suggesting that the effect of R:G ratio occurred consistently, but was relatively small. The

<sup>2</sup>Similar results were obtained in an earlier experiment with 16 participants. At that time, we had not yet refined the parameters for recording end-effector movements precisely. Nevertheless, the results of that experiment replicated those reported here, with two small, but significant, interaction terms involving viscosity coefficient—namely, viscosity coefficient  $\times$  ridge and viscosity-coefficient  $\times$  R:G ratio. Once again, the  $\eta^2$  values for the significant interaction terms were negligible (i.e., 0.009 and 0.002, respectively).

overall slope for the linear regression equation fit to the psychophysical function for  $\log_{10}$  perceived-roughness as a function of  $\log_{10}$  viscosity-coefficient, averaged over R:G ratio, is 0.88 with an  $r^2$  value of 0.994. No interaction terms were significant.

Once again, to disambiguate the effects of the correlated R:G ratio and groove width values, the  $\log_{10}$  normalized roughness estimates were plotted as a function of  $\log_{10}$  groove width for both ridge-to-groove ratios by ridge width. These are shown separately for each of the five viscosity-coefficients in Figure 5. In each viscosity-coefficient condition, the perceived-roughness estimates of the virtual gratings are consistently greater for the larger R:G ratio (open symbols) than for the smaller R:G ratio (closed symbols), whereas variations in groove width and ridge width have no apparent influence. These results replicate what was found in Experiment 1: the R:G ratio, rather than ridge or groove width, is the critical geometric factor.

When questioned at the end of the experiment about the cues used to estimate roughness magnitude, 11 of 12 participants mentioned that perceived-roughness was greater as the resistance to motion increased. A total of 7 participants also mentioned that roughness increased as the “bumpiness increased,” as the bumps became “bigger,” or as they became more “separated.”

**3.2.1 Probe Speed.** The corresponding mean probe speeds were calculated for each participant based on the PHANTOM output. A three-factor, within-subject ANOVA was performed on these data, the factors being viscosity-coefficient (five levels), ridge width (five levels), and R:G ratio (two levels). Of the three main effects, only ridge width was not statistically significant [for ridge width,  $F(2.21, 24.28) = 0.23$ ;  $p > 0.05$ ;  $\eta^2 = 0.001$ ]. For viscosity-coefficient,  $F(1.23, 13.48) = 21.98$ ,  $p < 0.0001$  and for R:G ratio,  $F(1, 11) = 53.65$ ,  $p < 0.0001$ . Corresponding  $\eta^2$  values were 0.338 and 0.115. Participants consistently moved the probe slower as both the viscosity-coefficient and ridge-to-groove ratio increased. In addition, there was a significant, but relatively minor contribution ( $\eta^2 = 0.012$ ), because of the interaction of viscosity-coefficient and R:G ratio,  $F(2.49, 27.35) = 3.52$ ,  $p < 0.05$ , which we will, therefore, not consider further. The mean speed for each of 12 participants is shown as a function of viscosity-coefficient in Figure 6.

To compare our results further with those obtained in the WingMan study [Klatzky and Lederman 2006], we determined Pearson correlations between the one kinematic variable we examined, speed, and the three microgeometric parameters of interest in both studies. These are reported in Table II. In this respect as well, the WingMan and PHANTOM results were not similar. Whereas all three correlations were statistically significant and large in the WingMan study, only the correlation between speed and R:G ratio was statistically significant in the current PHANTOM study; moreover, its magnitude was very small.

**3.2.2 Mean Resistive Force.** Given that participants tended to slow down as the viscosity-coefficient increased, one can ask whether the decrease in speed was sufficient to counter the increase in the viscosity-coefficient, thus yielding equivalent average resistive force. The mean resistive force was computed for each trial by taking the average of the instantaneous resistive force exerted by the Phantom over the duration of the trial. Across all trials and participants, the mean resistive force was 0.105 (SEM = 0.002)  $N$ , with a range of 0.51  $N$  (min = 0.008; max = 0.519). The mean resistive force is shown for each participant in Figure 7. The figure indicates that the mean resistive force consistently increased as the value of the viscosity-coefficient increased. Although several participants tended to slow their movement in the higher viscosity-coefficient conditions, overall the speed adjustment was minimal and insufficient to equalize the resistive forces experienced across different values of viscosity-coefficient.

Finally, we performed two multiple linear regressions that allowed us to examine both empirically and hypothesis-driven models, based on the results of our omnibus three-factor ANOVA and used to predict the mean  $\log_{10}$  normalized roughness estimates. The predictor variables included mean  $\log_{10}$  normalized

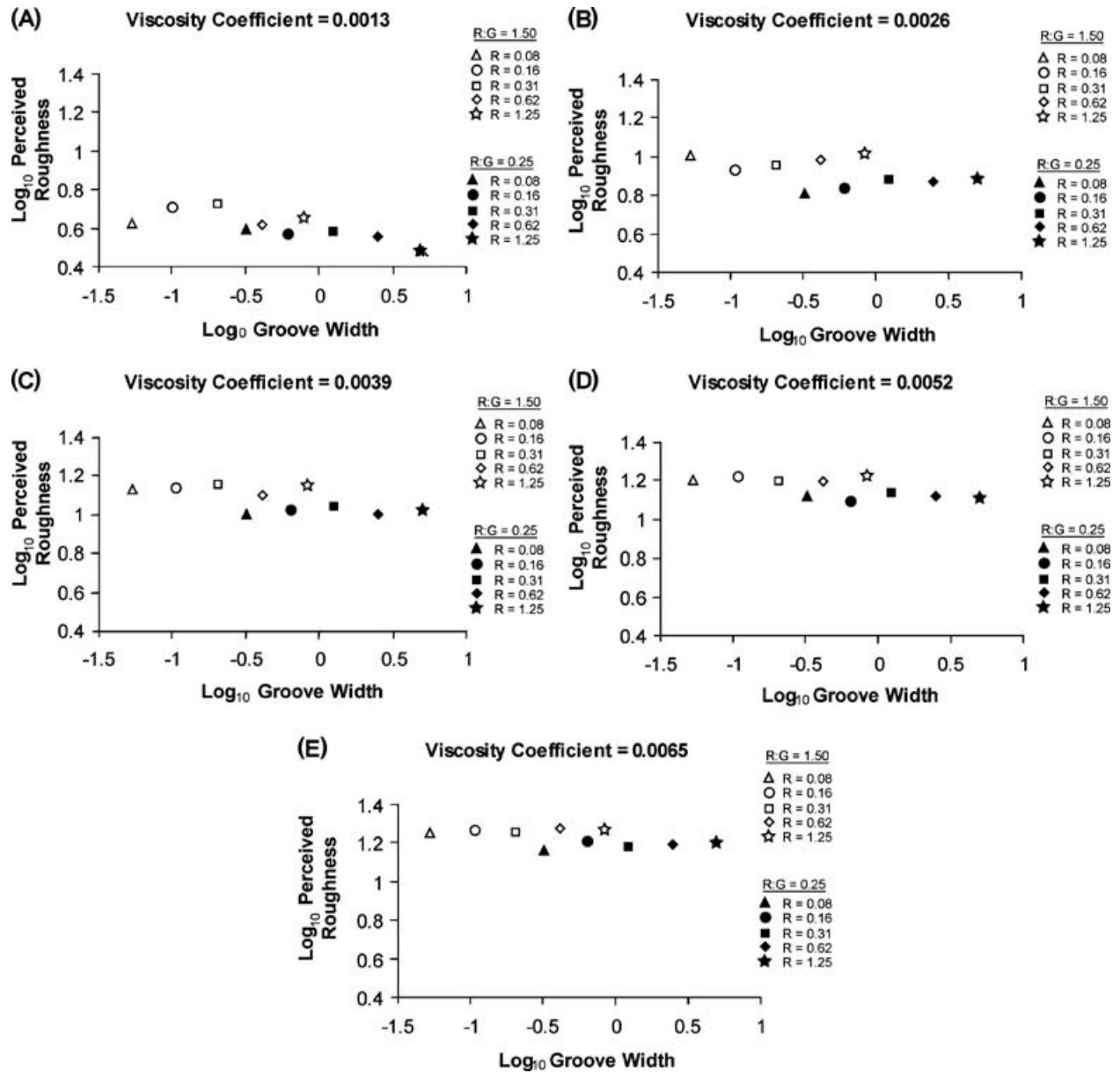


Fig. 5. Perceived-roughness (mean  $\text{log}_{10}$  normalized roughness magnitude estimates) as a function of  $\text{log}_{10}$  groove width, ridge width, and R:G ratio for five viscosity coefficient values, as shown in panels A–E.

resistive force,  $\text{log}_{10}$  viscosity-coefficient, and  $\text{log}_{10}$  ridge-to-groove ratio. The hypothesis-driven model adopted a stepwise procedure in which the following factors were entered one at a time in the following order: mean  $\text{log}_{10}$  force,  $\text{log}_{10}$  viscosity-coefficient, and  $\text{log}_{10}$  R:G ratio. This model allowed us to ask whether participants were indeed sensitive to variables other than mean resistive force, namely, the viscosity-coefficient and ridge-to-groove ratio. The hypothesis-driven model produced an  $R^2$  value of

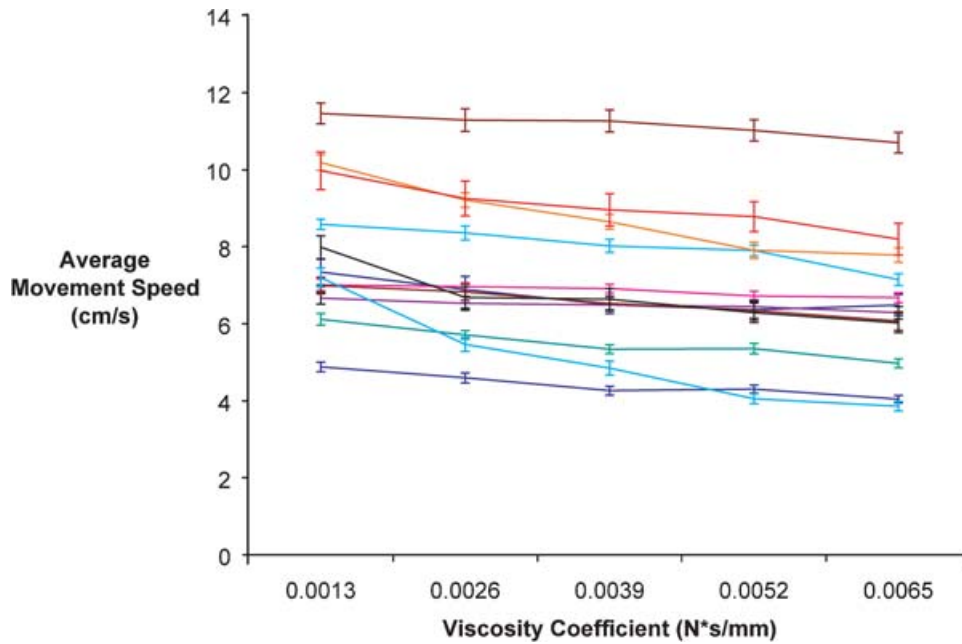


Fig. 6. Experiment 2: Effect of viscosity coefficient on average (mean) movement speed for 12 participants.

Table II. Experiment 2: Correlations (Pearson) between Mean Speed and Microgeometric Parameters of the Virtual Gratings

	Pearson Correlation	$p$ Value (two-tailed)	$N$
Speed and R:G ratio	-0.138	0.001	600
Speed and ridge width	0.002	0.965	600
Speed and groove width	0.006	0.889	600

0.533 when the  $\log_{10}$  viscosity-coefficient parameter was entered as the predictor variable.  $\log_{10}$  ridge-to-groove ratio accounted for an additional 0.028 ( $R^2 = 0.561$ ) and  $\log_{10}$  mean resistive force, only an additional 0.005 ( $R^2 = 0.566$ ). The effects of all three changes were significant at the 0.0001 level. Somewhat to our surprise, mean resistive force contributed only a very small effect to the roughness estimates. The second linear multiple regression analysis entered the same three variables into a model that optimized for the variance accounted. The standardized beta coefficients on  $\log_{10}$  mean force,  $\log_{10}$  viscosity-coefficient, and  $\log_{10}$  ridge-to-groove ratio were  $-0.172$ ,  $0.839$ , and  $0.281$ , respectively. Although each variable contributed a significant amount to optimizing the variance, the  $\log_{10}$  viscosity-coefficient and  $\log_{10}$  ridge-to-groove ratio predictor variables were more important than  $\log_{10}$  mean resistive force.

#### 4. GENERAL DISCUSSION

The results of Experiments 1 and 2 clearly confirm that the velocity-dependent viscosity-coefficient strongly influences participants' judgments of the roughness magnitude. More specifically, the perceived-roughness magnitude of virtual rectangular gratings increased with increases in the value of the viscosity-coefficient. Of all factors considered, the viscosity-coefficient, which was applied in the current experiments across the ridges of the virtual gratings, proved to be of primary importance.

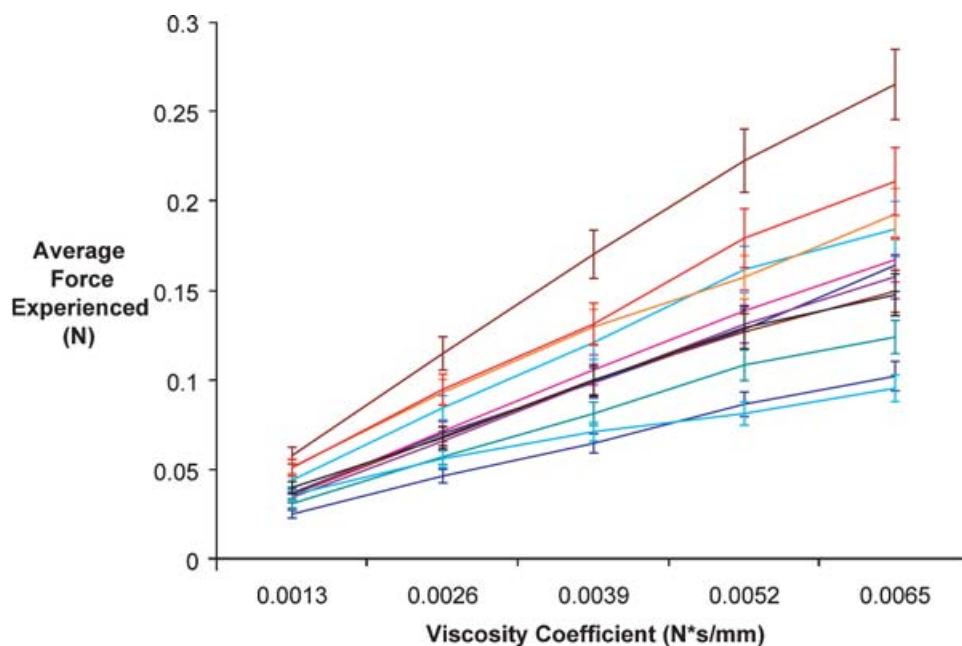


Fig. 7. Experiment 2: Effect of viscosity coefficient (N\*s/mm) on average (mean) force (N).

A secondary effect consisted of a slight increase in perceived roughness resulting from an increase in the value of R:G, the ridge-to-groove ratio. This pattern suggests a minor effect because of the spatial distribution of the viscosity coefficient across the gratings, namely, the proportion of resistance applied per cycle. It is possible that our participants interpreted changes in this parameter as changes in felt “rhythmicity.” Our reasoning is as follows. The ANOVA on the speed data showed neither a main effect of ridge width nor any interaction involving that factor. Statistically, this implies that participants maintained a constant speed for a given ridge-to-groove ratio, regardless of any change in the ridge width. We, therefore, infer that they did not attempt to compensate as a means of equating the duration of time spent on a ridge. Rather, as the ridge width was changed within a designated R:G level, participants would have experienced a constant rhythmic pulsing despite an increase in the tempo as the ridges became smaller.

Additional analyses revealed that neither the groove nor the ridge width significantly affected the magnitude of roughness experienced. We conclude that in the resistive environment created by using a viscosity-based algorithm in conjunction with the PHANTOM, parameters related to the microgeometry of the virtual gratings, do not substantially influence participants’ haptic estimates of roughness magnitude, relative to the substantial effect due to the viscosity coefficient.

Our results further indicate that for a given value of viscosity-coefficient, participants did not maintain a constant resistive force by reducing their exploration speed an equivalent amount. Although some participants reduced their movement speed slightly, this amount fell substantially short of what was required to maintain a constant force. The results of performing two multiple linear regressions, one based on a hypothesis-driven resistive-force model and the other based on an empirical variance-optimization model, confirmed that participants did not base their roughness estimates on the overall resistive forces generated during point contact with the virtual textures. We conclude that participants were sensitive to changes in the velocity-dependent viscosity coefficient, independent of the overall resistive force that was generated during exploration.

In our current research program on the perception of virtual textures, both the WingMan force-feedback mouse [Klatzky and Lederman 2006] and the PHANTOM Model 1.0 have been used to create virtual gratings based on resistive-force models. As the present experiment attempts to simulate the viscosity algorithm suggested by the WingMan, one might expect stimulus variables to have similar effects in the two environments. However, it is important to note that the two devices are operated differently and that the displays are very different in scale. Nevertheless, it is informative to compare the perceptual results. With the force-feedback mouse, judgments of perceived-roughness magnitude were strongly influenced by the microgeometry of the gratings, specifically, ridge width (cf., ridge-to-groove ratio and groove width). However, in the current study, the R:G ratio produced the sole microgeometric effect, and its magnitude was far subordinate to that of the viscosity coefficient, a nongeometric parameter.

It is intriguing to speculate that these differences stem from the activation of different mechanoreceptor populations, highlighting the need to understand the perception of virtual textures in terms of the interaction between the user and the device. Because the data in our companion study (this issue) showed that participants were relatively insensitive to the duration of pauses in resistance (i.e., virtual grooves), we suggested that the WingMan may elicit activation in slowly adapting mechanoreceptors that are sensitive to sustained stimulation across the virtual ridges. In addition, movement of the mouse over the base of the device produces real friction forces across the virtual groove and ridge areas. All four types of cutaneous mechanoreceptor units (i.e., slowly adapting Type I and II; fast-adapting Type I and II) respond to the application of tangential forces [Birznieks et al. 2001] and, thus, may play a role in coding virtual textures produced with the WingMan force-feedback mouse. In contrast, the PHANTOM does not produce any friction. To the extent that participants attended to the R:G ratio, they may have encoded temporal changes in resistance. As transient temporal information is sensed by fast-adapting mechanoreceptors (FA I, FA II units), it is possible that these types are preferentially activated in the current study.

Kinesthetic mechanoreceptors found in muscles, tendons, and joints may also differentially contribute to the haptic perception of virtual resistive textures in our companion studies. Consider first that the WingMan force-feedback mouse is limited to a very narrow range of lateral motions (22 and 18 mm in the x and y directions of the device, respectively), with such motions typically involving limited rotation about the wrist. Next consider that the mean mouse speed ranged from  $\sim 50$  to  $\sim 70$  mm/s, depending upon the specific experiment. Finally, consider that the viscosity coefficient remained constant in those experiments. In marked contrast, the range of motion permitted within the workspace of the PHANTOM was much greater and limited primarily by the size of the virtual stimuli. Thus, the width of the stimulus display was five-eight times larger than that of the WingMan (i.e., 110 and 178 mm in Experiments 1 and 2, respectively). The mean probe speed that was recorded in Experiment 2 was 71 mm/s, which is at the high end of the range obtained with the WingMan. In addition, participants rotated the PHANTOM probe about their shoulder as opposed to their wrist and were required to move the probe back and forth within two visually specified regions of the smooth sections of the grating. The generally higher speed of probe movements performed with greater spatial precision and the need to alter lateral force to counter the effect of manipulating the viscosity coefficient, may have caused participants to place greater emphasis on the kinesthetic inputs at the shoulder with the PHANTOM textures. Such differences between the two devices suggest that the neural representations based on sensory inputs from cutaneous and kinesthetic channels may be different. Our speculations concerning the possible underlying neural mechanisms, however, falls short of accounting for the psychophysical differences observed when the same stimulus parameters are manipulated using the two devices.

The importance of the viscosity coefficient in generating effective virtual gratings is further supported by earlier results [Weisenberger et al. 2000], which showed that based on a grating orientation task,

a damping-force model produced better tactile spatial acuity than a spring-force model. Here we show that variations in this single parameter can also produce a wide continuum of perceived-roughness. Increasing the value of the viscosity coefficient by a factor of 6.0 resulted in a systematic increase in perceived-roughness magnitude by a factor of 4.12.

In Part I, we presented results that offer promise for using inexpensive devices to produce virtual textures under unconstrained exploration. In that paper, we described a variety of techniques that have been used in the past to generate virtual textures. The current approach is more similar to the nongeometric technique used by Siira and Pai [1996] than to most other texture-rendering methods described in Part I. The experiments in Part II show that the velocity-dependent algorithm inspired by the experiments in Part I offers a very simple method for producing resistive virtual textures. Although our algorithm manipulates the velocity dependent viscosity coefficient, our data do not address whether this parameter is essential for altering perceived-roughness; for example, an acceleration-dependent resistance may work just as effectively. Future work will address such issues.

#### ACKNOWLEDGMENTS

This research was supported by grants to SL from the Natural Sciences and Engineering Research Council of Canada (NSERC) and the Institute for Robotics and Intelligent Systems (IRIS) Federal Centre of Excellence, and a PRECARN Scholar Award to CT.

#### REFERENCES

- BIRZNIKES, I., JENMALM, P., GOODWIN, A. W., AND JOHANSSON, R. S. 2001. Encoding of direction of fingertip forces by human tactile afferents. *Journal of Neuroscience* 21, 8222–8237.
- BLAKE, D. T., HSIAO, S. S., AND JOHNSON, K. O. 1997. Neural coding mechanisms in tactile pattern recognition: The relative contributions of slowly and rapidly adapting mechanoreceptors to perceived-roughness. *Journal of Neuroscience* 17, 7480–7489.
- BRYDEN, M. P. 1977. Measuring handedness with questionnaires. *Neuropsychologia* 15, 617–624.
- CAMPION, G. AND HAYWARD, V. 2005. Fundamental limits in the rendering of virtual haptic textures. In *Proceedings of the 1st Joint Eurohaptics Conference and Symposium on Haptic Interfaces for Virtual Environment and Teleoperator Systems*. IEEE Computer Society, Los Alamitos, CA, 263–270.
- CHOI, S. AND TAN, H. Z. 2002. An analysis of perceptual instability during haptic texture rendering. In *ASME Proceedings of the 10th International Symposium on Haptic Interfaces for Virtual Environment and Teleoperator Systems*, 129–136.
- CHOI, S. AND TAN, H. Z. 2003. An experimental study of perceived instability during haptic texture rendering: Effect of collision detection algorithm. In *IEEE Proceedings of the 11th International Symposium on Haptic Interfaces for Virtual Environment and Teleoperator Systems*. 197–204.
- CONNOR, C. E. AND JOHNSON, K. O. 1992. Neural coding of tactile texture: Comparison of spatial and temporal mechanisms for roughness perception. *Journal of Neuroscience* 12, 9, 3414–3426.
- CONNOR, C. E., HSIAO, S. S., PHILLIPS, J. R., AND JOHNSON, K. O. 1990. Tactile roughness: Neural codes that account for psychophysical magnitude estimates. *Journal of Neuroscience* 10, 3823–3836.
- HOLLINS, M. AND RISNER, S. R. 2000. Evidence for the duplex theory of tactile texture perception. *Perception & Psychophysics* 62, 4, 695–705.
- HOLLINS, M., BENSMAIA, S. J., AND RISNER, S. R. 1998. The duplex theory of tactile texture perception. In *Proceedings of the fourteenth Annual Meeting of the International Society for Psychophysics*, 115–121.
- KATZ, D. 1925/1989. In *The World of Touch*, L. E. Krueger, Ed./Transl. Lawrence Erlbaum, Hillsdale, New Jersey.
- KLATZKY, R. L. AND LEDERMAN, S. J. 1999. Tactile roughness perception with a rigid link from surface to skin. *Perception & Psychophysics* 61, 4, 591–607.
- KLATZKY, R. L. AND LEDERMAN, S. J. 2002. Haptic perception. In *Encyclopedia of Cognitive Science*, L. Nadel, Ed. Macmillan Ref. Ltd, London, 508–512.
- KLATZKY, R. L. AND LEDERMAN, S. J. 2006. Perceived-roughness of resistive virtual textures: I. Rendering by a force-feedback mouse. *ACM Transactions on Applied Perception* 3, 1, 1–14.
- KLATZKY, R. L., LEDERMAN, S. J., HAMILTON, C., GRINDLEY, M., AND SWENDSEN, R. 2003. Feeling textures through a probe: Effects of probe/plate geometry and exploratory factors. *Perception & Psychophysics*, 65, 4, 613–631.

- LAMOTTE, R. H. AND SRINIVASAN, M. A. 1991. Surface microgeometry: Tactile perception and neural encoding. In *Information Processing in the Somatosensory System*, O. Franzen and J. Westman, Eds. Macmillan, New York, 49–58.
- LEDERMAN, S. J. 1983. Tactual roughness perception: Spatial and temporal determinants. *Canadian Journal of Psychology* 37, 498–511.
- LEDERMAN, S. J., KLATZKY, R. L., HAMILTON, C., AND RAMSAY, G. I. 1999. Perceiving roughness via a rigid probe: Effects of exploration speed and mode of touch. *Haptics-e (The Electronic Journal of Haptics Research)* 1, 1, 1–20.
- LEDERMAN, S. J., KLATZKY, R. L., HAMILTON, C., AND GRINDLEY, M. 2000. Perceiving surface roughness through a probe: effects of applied force and probe diameter. In *Proceedings of the American Society for Mechanical Engineers, Dynamic Systems and Control Division 69-2*, 1065–1071.
- SHIRA, J. AND PAI, D. K. 1996. Haptic Textures—A Stochastic Approach. In *IEEE International Conference on Robotics and Automation (Minneapolis)*, 557–562.
- STEVENS, S. S. AND HARRIS, J. R. 1962. The scaling of subjective roughness and smoothness. *Journal of Experimental Psychology: General* 64, 5, 489–494.
- TAYLOR, M. M. AND LEDERMAN, S. J. 1975. Tactile perception of grooved surfaces: A model and the effect of friction. *Perception & Psychophysics* 17, 1, 23–36.
- WEISENBERGER, J. M., KRIER, M. J., AND RINKER, M. A. 2000. Judging the orientation of sinusoidal and square-wave gratings via 2-DOF and 3-DOF haptic interfaces. *Haptics-e* 1, 4, 1–20.
- YOSHIOKA, T., GIBB, B., DORSCH, A. K., HSIAO, S. S., AND JOHNSON, K. O. 2001. Neural coding mechanisms underlying perceived roughness of finely textured surfaces. *Journal of Neuroscience* 21, 17, 6905–6916.

Received March 2005; revised August 2005; accepted November 2005